IEEE Journal of Microwaves

Received 27 October 2021; revised 13 February 2022; accepted 20 April 2022. Date of publication 16 May 2022; date of current version 7 July 2022.

Digital Object Identifier 10.1109/JMW.2022.3170060

Low Profile Dielectric Rod Tuned Reconfigurable Band Pass Filters

SRIPARNA DE [1] (Graduate Student Member, IEEE), SHIBAN K. KOUL [1] (Life Fellow, IEEE), AND KAMAL K. SAMANTA [2] (Senior Member, IEEE)

(Regular Paper)

[1]Centre for Applied Research in Electronics, IIT Delhi, New Delhi 110016, India
[2]AMWT Ltd., HA8 5BB London, U.K.

CORRESPONDING AUTHOR: Sriparna De (e-mail: de.thesriparna@gmail.com).

ABSTRACT A novel low profile mechanical tuning technique is introduced in this paper to change the center frequency of substrate integrated waveguide (SIW) based reconfigurable bandpass filters (BPF), by loading dielectric rods of different permittivity in resonant cavities and coupling apertures. The technique is simple, cost-effective (rods are machined from conventional substrates), and the same physical structure provides a wide frequency tuning. First, the tunability of center frequency of the SIW cavity resonator is theoretically explained and then estimated with the help of full-wave 3D EM simulator and electrical equivalent circuit. This concept is extended to the tuning of coupled resonator BPF loaded with dielectric rods followed by the analysis of maintaining constant bandwidth. Following the analysis technique, the tunability concept is studied for different arrangements of dielectric rods inside the SIW BPFs. The characteristics of the fabricated filters are experimentally validated. It is shown that center frequency tunability can be achieved by simply varying the permittivity of all the dielectric rods simultaneously. The proposed technique is further extended for obtaining wider tunability and constant bandwidth by using dielectric rods of dissimilar permittivities from a look up table. These designs demonstrate a simple and cost-effective passive tuning technique achieving high Q-factors in the range of 102–210.5, lowest insertion loss <2dB above 10 GHz, and wide tuning bandwidth in X-band. The reconfigurable filters are developed for advanced high-speed, long-distance, and fixed wireless connectivity in a rural area at a low cost. The technique can also be used for temperature compensation and overcoming fabrication uncertainty.

INDEX TERMS Band pass filter (BPF), dielectric rod, reconfigurable, substrate integrated waveguide (SIW).

I. INTRODUCTION

Integrated bandpass filters (BPF) are key elements for achieving compactness and performance in an RF module [1]. Further, reconfigurable filters are important in dynamic spectrum management in cognitive and software-define-radio design platforms and phase-controlled systems for both military and civilian applications. In a multi-band communication system, wideband tracking receivers, and multichannel front-end modules (FEM) for radar, and mobile communication systems, reconfigurable filter plays significant role. In advanced point-to-multipoint (P2MP) and point-to-point (P2P) radios (including 5G) and especially for fixed and affordable high-speed internet connection in the hard-to-reach areas, such as small islands and rural areas, multi-channel FDM (frequency division multiplex) is essential. The module should provide high data rate at a long range with reduced power consumption and ensuring that customer premise equipment (CPE) is affordable and easier to be installed in a remote area where power is limited or non-existent. As depicted in Fig. 1, the central node i.e., the base station works as the FDM transmitter which transmits one frequency to one user and other frequency to another user. Different CPEs are attached to different users that require various transmit/receive filters operating at different frequency bands that are pre-decided and fixed. To avoid crosstalk between these users, network providers need to manufacture BPF of a large variety for various CPE operating at different frequency bands/channels, which makes the components inventory management and CPE very

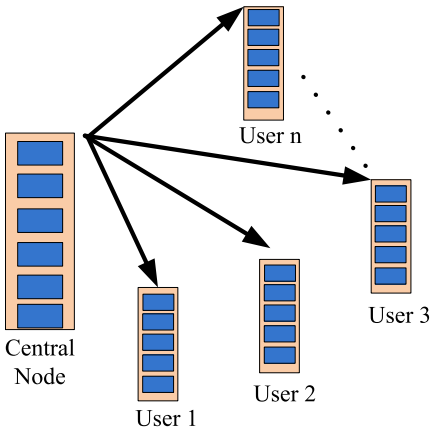

FIGURE 1. **Point to multi-point (P2MP) communication.**

expensive. Alternatively, active tuned filters are used which require additional complex DC bias circuit, which not only suffers from component's size, complexity and reliability penalties but also makes the component/solution more expensive and power consuming.

The proposed mechanical tuning technique is used to design the filters for CPEs where same fabricated structure can be used at fixed but different frequencies with different dielectric rod loading. The filter is reconfigured to different channel frequencies for different CPEs with passive tuning. Although mechanical tuning is slower than electrical tuning. But in this application, switching speed is not the main concern. Since once the design is reconfigured, it remains in that configuration for that CPE. In industry, this solution makes the inventory management cost effective and easier for the network providers.

Most commonly available frequency tuning techniques include electrical tuning using semiconductor varactor diodes [2]–[6] and PIN diodes [7]–[11], magnetic tuning using ferrite materials mainly yttrium-iron-garnet (YIG) [12]–[17], ferroelectric materials [18]–[23] and using micro-electromechanical systems (MEMS) [24]–[29]. The proposed tuning technique in this paper is demonstrated based on SIW technology. In comparison to planar transmission lines such as microstrip and coplanar waveguides, SIW exhibits high-power handling capacity and is easily integrable with other planar transmission lines and active devices. SIW also inherits the characteristics of rectangular waveguides and planar transmission lines [30]. Different electronically tunable SIW filters are already reported using PIN diodes [31], MEMS devices [32], varactor diode [33], ferroelectric ceramic substrate [34], ferrite [35]–[36], plasma [37]. Discrete mechanical tuning is proposed in [38]–[42] using metallic screw/flaps/liquid metal perturbing posts. BPFs using SIW cavity loaded with expensive dielectric resonators oscillators (DRO) have been explored by many researchers [43]–[45], which are focused on miniaturization.

To the best of our knowledge, tunability of SIW bandpass filters incorporating position, dimensions and dielectric permittivity of dielectric rods has not been reported so far. In the proposed technique, a wide range of frequency tuning can be achieved using the same physical structure, only by varying dielectric constant and/or the number of rods, machined from low-cost commonly used dielectric substrates. This eliminates the use of any external DC bias circuitry, parasitic effects, and related frequency limitation, and reduces power consumption, which are main drawbacks of active tuning techniques [31]–[36]. These rods are easy to manufacture with in-house facilities and can be easily integrated with SIW planar circuit. It causes minimum field perturbation, and hence better insertion loss and higher Q-factor values can be achieved over wider bandwidth, as compared to conventional metallic screws/flaps [38]–[41]. The proposed technique has been developed for industrial applications, where keeping the fabricated physical structure of the BPF same, the frequency can be reconfigured for optimum performance and matching with the required channel or band of a multichannel or multi-band modern systems with high compactness. For more applications such as in compensating fabrication uncertainty, on the field, and on-tower tuning and performance optimization, passive tuning with manual changing of the single or stacked dielectric rod can be performed.

The paper is arranged as follows: Section II illustrates the tunability mechanism of dielectric rod loaded SIW cavity resonator and then it is expanded to the analysis of the designed iris window SIW BPF. Section III demonstrates two techniques for realizing reconfigurable BPF. First, a simple on-field reconfigurable BPF is demonstrated where relative permittivity of all the dielectric rods is changed simultaneously (without look up table), to tune the center frequency of the filter, for enabling easy on-field or on-tower tunning. The proposed technique is then extended further for the less cost sensitive applications, but to achieve wider tunability (16.9%), constant bandwidth and higher out of band rejection by using dielectric rods of different permittivities at the center of the resonant cavities and the coupling apertures. These relative permittivities are calculated to maintain a constant bandwidth with the tuning of center frequency and according to that calculation, a lookup table is followed to show better tunability in terms of bandwidth and rejection. The paper is concluded in Section IV.

II. THEORY OF DIELECTRIC ROD TUNED SIW FILTER

This section first describes the tuning mechanism of the SIW cavity, loaded with a dielectric rod followed by the analysis of reconfigurable SIW BPF. The proposed tuning technique is applied to the cavity first and then this fundamental block of iris window coupled filter is used to design the final reconfigurable filter. The theory of tuning the center frequency is developed in this section.

A. TUNING OF SIW CAVITY RESONATOR

Cavity resonator is the basic building block of iris window coupled resonator BPF. This part discusses how a dielectric

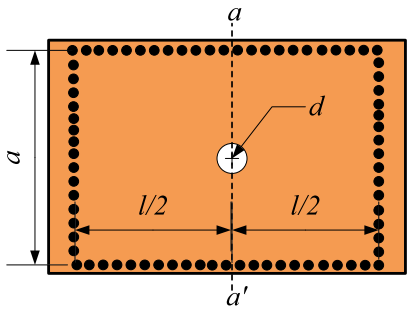

FIGURE 2. Layout of SIW cavity resonator loaded with dielectric rod.

rod can be used to tune the resonant frequency of a conventional SIW cavity resonator. The proposed theory is validated experimentally also in the next half, by fabricating a cavity resonator with dielectric rod loading.

1) TUNING MECHANISM

The resonant frequency of the SIW cavity (without dielectric rod) can be calculated as that of the rectangular cavity, since the propagation of a TE_{10}-like mode in SIW is like the TE_{10} mode of a rectangular waveguide. The effective width '*a*' determines the frequency band of the guide and then the length of the cavity '*l*' mainly decides the resonant frequency of the cavity. Fig. 2 outlines a conventional SIW resonator loaded with a dielectric rod of diameter *'d'*. There is an air hole at the center of the cavity where a dielectric rod of different relative permittivity is placed turn by turn to show tunability in the resonant frequency of the cavity resonator. The height of the rod is the same as that of the substrate. It is aligned parallel to the electric field.

Theoretical analysis to determine the characteristic equation for the structure shown in Fig. 2 is presented in this section. Mathematically, the resonant frequency of a cavity can be calculated either by solving Maxwell's equation or by analyzing the electrical equivalent circuit of the cavity resonator. Analytically solving Maxwell's equation may be quite complicated and it may yield some redundant solutions also. Hence the analysis of the electrical equivalent circuit is followed to calculate the resonant frequency of the SIW cavity resonator loaded with a dielectric rod.

At the cavity resonance frequency, a simple transmission line theory is used to derive the characteristic equation for which higher-order modes are ignored. In the equivalent circuit, the SIW section of fixed width is assumed as a transmission line working at the corresponding frequency of operation, having propagation constant and characteristic impedance corresponding to that of the SIW. The solution of the equation yields the resonant frequency of the SIW cavity resonator loaded with a dielectric rod. The complete analysis assumes that the rod is placed at the center of the cavity (along the length). Hence the physical structure of the resonator is symmetric with reference to plane *aa*' in Fig. 2. According to the field pattern, the reference plane aa' satisfies the boundary

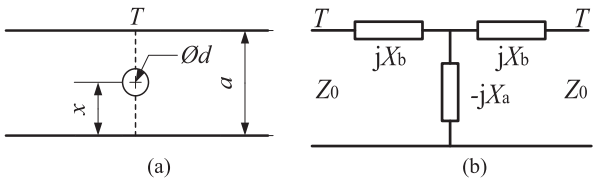

FIGURE 3. (a) Top view of dielectric rod inside the rectangular waveguide and (b) Its equivalent circuit [48].

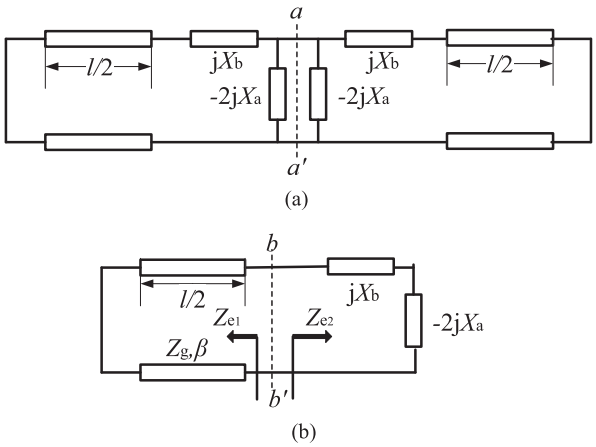

FIGURE 4. (a) Equivalent transmission line model of SIW cavity resonator loaded with a dielectric rod and (b) Left half of the equivalent circuit with aa' as open circuit at resonance.

condition of a magnetic wall; hence the plane can be represented as an open circuit in the corresponding equivalent circuit. The equivalent circuit of a dielectric rod inside the rectangular waveguide is depicted in Fig. 3 which is applicable in the wavelength range $2a>\lambda>a$, and for the central cylinder in the wider range $2a>\lambda>2a/3$ [48].

In the equivalent transmission line model of Fig. 4(a), SIW sections on both sides of the dielectric rod are represented by a transmission line of length *l*/2 and the dielectric rod is replaced by its corresponding equivalent circuit depicted in Fig. 3. Since the circuit of Fig. 4(a) is an open circuit at reference plane *aa*', the characteristic equation of one half of the circuit will be the same as that of the complete circuit at resonance. Hence the characteristic equation is derived from the circuit of Fig. 4(b) which is half of the circuit shown in Fig. 4(a).

From transmission line theory, the impedance looking from the reference plane *bb'* towards the short-circuited SIW section of length *l*/2 is given by—

$$Z_{e1} = \mathrm{j}Z_g \tan\left(\frac{\beta l}{2}\right) \tag{1}$$

And the impedance looking on the other side from reference plane *bb'* is given by —

$$Z_{e2} = -2\mathrm{j}X_a + \mathrm{j}X_b \tag{2}$$

The resonance condition of the transmission line requires that at any point on the line, the sum of the imaginary part of the input impedance seen looking to either side must be

zero [49] i.e.,

$$\mathrm{Im}\,(Z_{e1} + Z_{e2}) = 0 \tag{3}$$

$$\frac{1}{2}\tan\left(\frac{\beta l}{2}\right) - \left(\frac{Xa}{Zg} - \frac{Xb}{2Zg}\right) = 0 \tag{4}$$

where Z_g is the guide impedance and β is the propagation constant of the TE_{10}-like mode of SIW transmission line section and X_a, X_b is the reactance associated with the dielectric rod as depicted in Fig. 3. From [48], the characteristic equation of the waveguide cavity with dielectric rod is calculated as —

$$\frac{1}{2}\tan\left(\frac{\pi l}{v}\left(f^2 - fc^2\right)^2\right) - \frac{a}{2\lambda}\left(1 - \left(\frac{\lambda}{2a}\right)\right)^{\frac{1}{2}} \cos ec^2\left(\frac{\pi x}{a}\right)$$
$$\left[\frac{2\lambda^2}{(\varepsilon-1)\pi^2 d^2} - \frac{(\varepsilon-3)}{4(\varepsilon-1)} - \ln\left(\frac{4a}{\pi d}\sin\left(\frac{\pi x}{a}\right)\right)\right.$$
$$\left. +2\sin^2\left(\frac{\pi x}{a}\right) - 2\sum_{n=2}^{\infty}\sin^2\left(\frac{n\pi x}{a}\right)\left[\frac{1}{\left(n^2 - \left(\frac{2a}{\lambda}\right)^2\right)^{\frac{1}{2}}} - \frac{1}{n}\right]\right] = 0 \tag{5}$$

The solution of (5) gives the theoretical resonant frequency of the dielectric rod loaded cavity. This resonant frequency is a function of *d/a, x/a* and ε ($\varepsilon_{rod}/\varepsilon_{substrate.}$). Thus, by varying diameter *d,* position *x* and ε_{rod}, tunability in resonant frequency can be achieved.

2) VERIFICATION OF THE PROPOSED TECHNIQUE

Considering the frequency of operation at X-band, SIW cavity resonator is designed in Ansys HFSS using Rogers 5880B substrate of height 0.508 mm and relative permittivity of 2.2 with a =15.85 mm and l=0.6a. The diameter of the via holes and separation between them is set to 0.8 mm and 1.6 mm, respectively. Diameter of the dielectric rod, d=0.1a and x=0.5a. The permittivity of the rod is varied as 8, 12, 16 and 20 to study resonant frequency tunability of the SIW cavity resonator mathematically. For the fixed dimensions of the cavity, diameter and position of the dielectric rod, the plot of the variation of normalized impedance, for different values of the relative permittivity of the dielectric rod is shown in Fig. 5 for X-band. The 0.5tan(βl/2) plot shown in the blue line intersects at different reactance curves corresponding to different TE_{101} mode resonant frequencies. Fig. 5 shows that the resonant frequency of the dielectric rod loaded SIW cavity decreases with an increase in ε_{rod}. This analysis is done considering all the dielectric rods as lossless material.

Fig. 6 shows the variations of resonant frequency with respect to ε_{rod} for three different values of *d/a*. The analysis is done considering *d/a* up to 0.15 to avoid resonance within dielectric rods according to [48]. It is depicted that analytically calculated values of resonant frequencies match well with the simulated one. It is also demonstrated that resonant frequency reduces with an increase in relative permittivity of the dielectric rod for a given *d/a*. It is also evident that the slope of curves increases with an increase in *d/a* ratio which means that tuning of resonant frequency is more sensitive for a higher ratio of *d/a*.

An SIW cavity resonator at X-band is fabricated on 20 mil Rogers 5880B substrate to validate the theory of tuning. Microstrip lines are used to excite the resonator as shown in Fig. 7(a). Dimensions of the resonator are given in Table 1. Dielectric rods are made using Laser cutting from Rogers 6010 (ε_{rod} =10.2, tan δ = 0.0023) and Rogers 5880B (ε_{rod} =2.2, tan δ=0.0009) substrates.

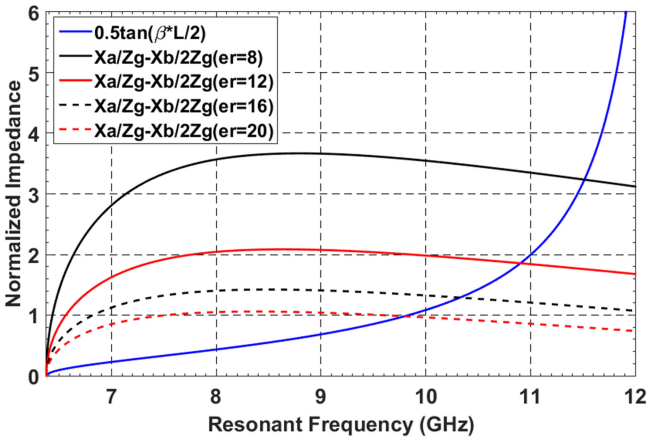

FIGURE 5. Normalized impedance of SIW cavity resonator with respect to change in relative permittivity of dielectric rod and resonant frequency.

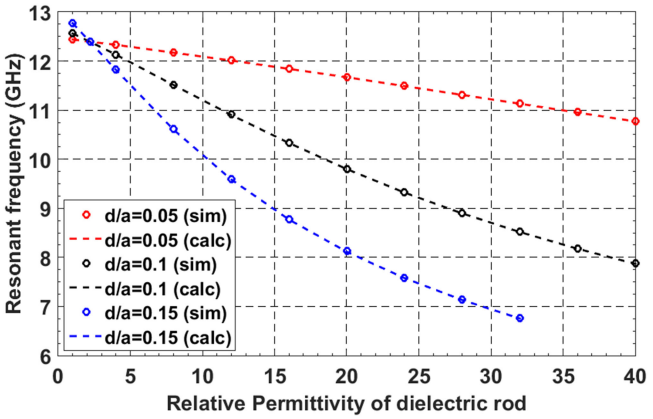

FIGURE 6. Variation of resonant frequency with respect to relative permittivity and diameter of dielectric rod for l=0.6a.

TABLE 1. Geometrical Parameters of the Cavity [Unit: mm]

Symbol	Value	Symbol	Value
W_m	1.56	s	0.8
W_t	5.43	p	1.6
Lt	13.4	d	2
l	8.7	W_{ap1}	7

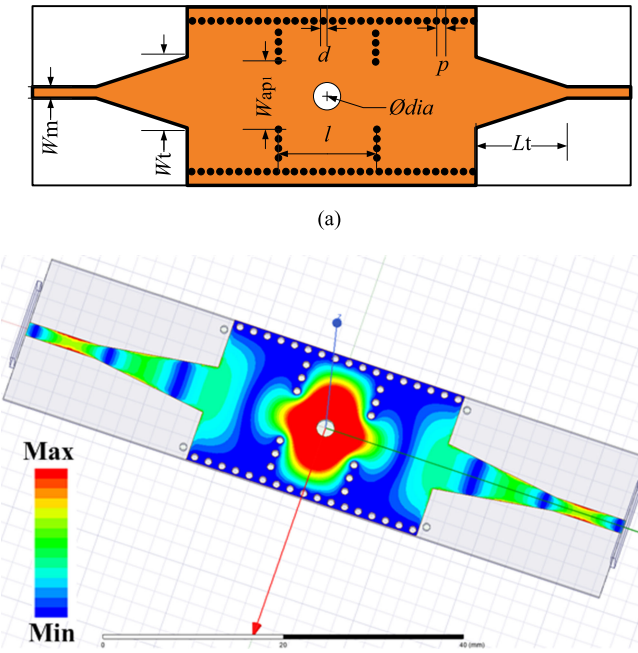

FIGURE 7. (a) Layout and (b) Electric field distribution of SIW cavity resonator loaded with dielectric rod.

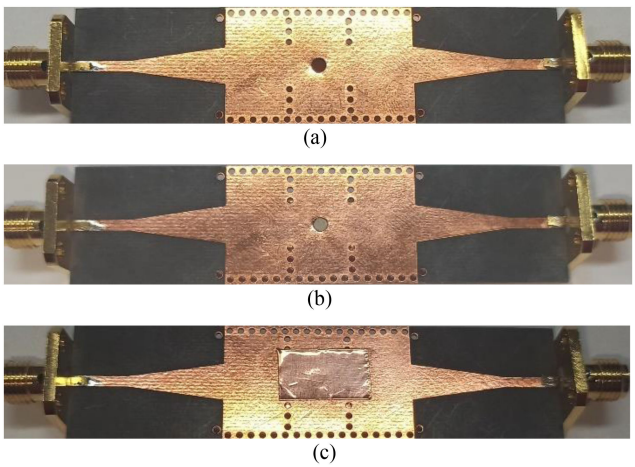

FIGURE 8. Photograph of reconfigurable SIW resonator (a) without dielectric rod, (b) with rod, and (c) Top view with rods covered with copper tape (Dimension: 30 mm × 18 mm).

First, the cavity resonator without any rod is measured in VNA. Then rods of ε_{rod} equal to 2.2 and 10.2 are inserted respectively and they are covered with copper tapes at top and bottom as presented in Fig. 8. Then measurements are taken for these two cases respectively. A metallic screw is also inserted to compare its loss characteristics with that of the dielectric rods. All the measured results are compared in Fig. 9. Fig. 9 depicts a total tunability of resonant frequency from 10 GHz to 11.9 GHz. So, 17.35% tunability can be achieved only with a small variation of ε_{rod} from 1 to 10.

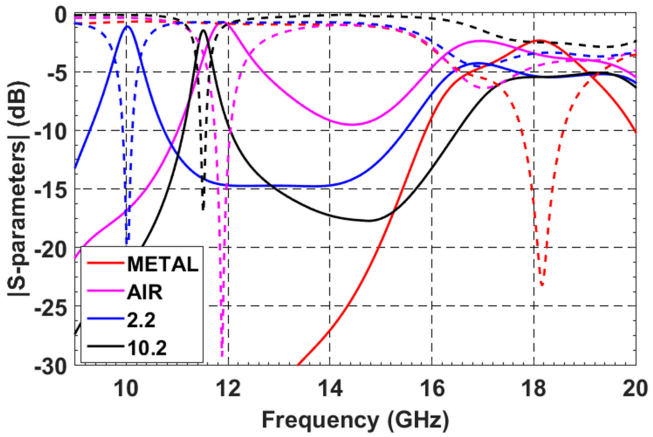

FIGURE 9. Return loss (dotted line) and insertion loss (solid line) of SIW cavity resonator with metallic screw and different dielectric rods.

TABLE 2. Extracted Q-Factor of the Designed Cavity Resonator

Rod	ε_{rod}	tan δ^*	f_0 (GHz)	FBW (%)	Q_u
Air	1	0	11.9	0.59	162.43
5880B	2.2	0.0009	11.58	0.31	145.99
6010	10.2	0.0023	10	0.51	82.41
Metal	-	0	18.11	2.38	32.10

*tan δ = dielectric loss tangent, so tan δ for metal is 0.

Unloaded Q-factors (Q_u) of the cavity resonator at all the resonant frequencies for each of the dielectric rod and metallic screw are extracted from measured results of Fig. 9, using the technique given in [49] and they are summarized in Table 2. From Table 2, it is observed that Q_u of dielectric rods is more than that of the metallic screw. This implies that dielectric rods are less lossy than metallic screws which are generally used in conventional passive tuning techniques. Permittivity and loss tangent tolerances are also checked in simulation to characterize the dielectric rods. $\varepsilon_{rod} \pm 1$ changes the resonant frequency of the cavity by ∼0.3-0.4%. Whereas change in loss tangent of the material by tan δ ±0.001 barely affects the resonant frequency and insertion loss of the resonator.

B. TUNING OF IRIS WINDOW SIW BPF

This section employs the dielectric rods inside SIW BPF for further extension of the proposed tuning concept in coupled resonator filter. The reconfigurable cavity resonators are coupled through iris windows to design SIW BPF. The presence of dielectric rods modifies the length calculation of the cavities for the iris window BPF. So, the next section gives an idea of that modification, followed by the analysis of the center frequency tuned SIW BPF. It also discusses how these tuning elements can be used to maintain the constant bandwidth of the filter while tuning the center frequency.

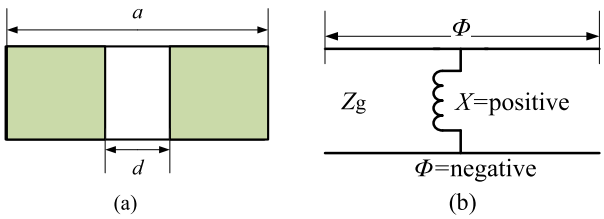

FIGURE 10. Cross-sectional view of an inductive window inside the rectangular waveguide and its equivalent K-inverter network [48].

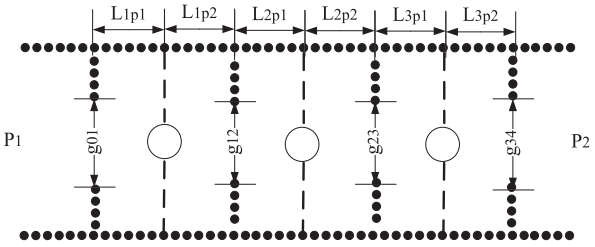

FIGURE 11. The layout of dielectric rods loaded iris window SIW filter.

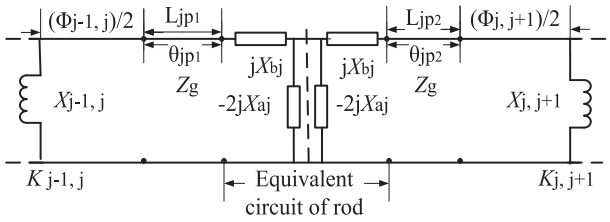

FIGURE 12. Equivalent circuit of an SIW cavity resonator in the BPF, loaded with dielectric rod and K-inverters on both sides.

1) MODIFICATION IN THE STANDARD DESIGN PROCESS OF IRIS WINDOW SIW BPF

For designing SIW BPF, the width of the iris window calculation follows standard procedure [50]. However, the length calculation for the cavities is modified due to the presence of a dielectric rod inside the cavity. The equivalent circuit of an iris window inside a rectangular waveguide can act as a K-inverter as depicted in Fig. 10. Now, the effect of the K-inverter is considered to calculate the new physical length of the SIW cavity resonators which are coupled through the inductive window as shown in Fig. 11. The equivalent circuit of one of the cavities, loaded with a dielectric rod and two K-inverters is presented in Fig. 12, which is considered for further calculation.

With reference to the analysis of the SIW cavity resonator, loaded with dielectric rod described in the previous section, the magnetic wall is formed along with the dielectric rod position in each cavity of the BPF. So, the dotted line in Fig. 12 represents an open circuit. Then length calculation of either half of each cavity is modified as follows. Hence it can be written that—

$$\alpha_j = \tan^{-1}\left[2\left(\frac{X_{aj}}{Zg} - \frac{X_{bj}}{2Zg}\right)\right] \tag{6}$$

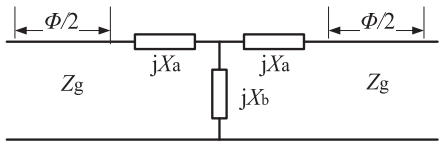

FIGURE 13. Equivalent K-inverter circuit of iris window with finite thickness [50].

Where $\left[\left(\frac{X_{aj}}{Zg} - \frac{X_{bj}}{2Zg}\right)\right]$ is calculated at the center frequency.

$$\theta_{jP1} = \alpha_j - \frac{1}{2}\tan^{-1}\left(\frac{2X_{j-1,j}}{Z_g}\right)$$
$$\theta_{jP2} = \alpha_j - \frac{1}{2}\tan^{-1}\left(\frac{2X_{j,j+1}}{Z_g}\right) \tag{7}$$

Where $\left(\frac{X_{j-1,j}}{Z_g}\right)$ and $\left(\frac{X_{j,j+1}}{Z_g}\right)$ are marked in the equivalent circuit and their values are given in [50].

Hence the total physical length of individual cavity resonator considering the effect of K-inverter is calculated as—

$$L_j = L'_{jP1} + L'_{jP2}$$
$$\text{where } L'_{jP1} = \theta_{jP1} * \frac{\lambda_{go}}{2\pi}$$
$$\text{and } L'_{jP2} = \theta_{jP2} * \frac{\lambda_{go}}{2\pi} \tag{8}$$

However, for the finite thickness of the iris, the equivalent circuit of Fig. 10(b) is modified by a T-network as shown in Fig. 13. Equations of the above K-inverter circuit are given in [50]. Accordingly, the effective physical length will have to be modified. The above analysis shows the modifications in the standard iris window filter design process, due to the presence of a dielectric rod in the cavity. In the next section, center frequency tuning is illustrated analytically by changing the dielectric constant and diameter of the dielectric rods in the designed SIW BPF.

2) ANALYSIS OF THE PROPOSED SIW BPF

Once the SIW BPF is designed as shown in Fig. 11, for a particular dimension and ε_{rod}, any change in dielectric constant and/or diameter of the rod results in a change in the center frequency of BPF, and thus tuning can be achieved. Calculating the center frequency is a bit complex since the BPF consists of multiple resonators resonating at the center frequency. For tuning of BPF, all the resonators are needed to be tuned simultaneously.

To get an idea of the new center frequency, only the central resonator is considered because of its symmetricity in the geometrical configuration as well as simplicity in the analysis. Other resonators will also resonate at the tuned center frequency. Due to symmetricity, the characteristic equation of one half of that circuit will be the same as that of the complete circuit at resonance. So, a similar approach of the equivalent circuit of Fig. 4 is applied here also. A little modification of an

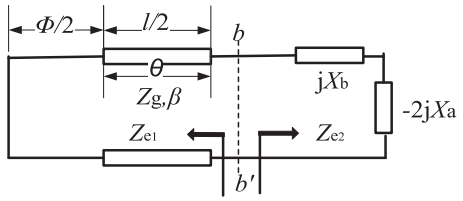

FIGURE 14. Equivalent circuit of modified cavity resonator coupled with iris window.

TABLE 3. Geometrical Parameters of the Designed BPF [Unit: mm]

Symbol	Value	Symbol	Value
a	15.85	d	0.1a
L_{1p1}	4.867	g_{01}	6.367
L_{2p1}	5.77	g_{12}	4.035
L_{3p1}	5.77	g_{23}	4.035
L_{1p2}	5.77	g_{34}	6.367
L_{2p2}	5.77	L_{3p2}	4.867

additional electrical length of $\varphi/2$ because of the iris window is considered as shown in Fig. 14.

Hence both effect of the dielectric rod, as well as the coupling window, is considered here. The characteristic equation is modified as—

$$\mathrm{Im}\left[jZ_g\tan\left(\theta-\frac{\varphi}{2}\right)+jX_b-j2X_a\right]=0$$

$$\frac{1}{2}\tan\left(\frac{\pi}{v}\left(f^2-fc^2\right)^{\frac{1}{2}}+\frac{1}{2}\tan^{-1}\left(\frac{2X_{j-1,j}}{Zg}\right)\right)-\left[\frac{X_a}{Zg}-\frac{X_b}{2Zg}\right]=0 \quad (9)$$

The solution of this characteristic equation yields the new approximate center frequency of the BPF. The sensitivity of the center frequency f with respect to d, can be done by differentiating (9).

Based on the design equations of the above sections, a 0.5 dB 3rd order Chebyshev iris window SIW BPF with dielectric rod is designed at 9 GHz with a BW of 350 MHz using Rogers 5880B substrate of height 0.508 mm and relative permittivity of 2.2. Dimensions of the BPF as calculated theoretically for $\varepsilon_{rod}=16$, are given in Table 3.

In the above designed BPF, ε_{rod} is varied from 1 to 32 for three different d/a ratios. The corresponding center frequency is calculated theoretically and simulated as well. The plots are shown in Fig. 15. It is demonstrated that for any particular d/a ratio, center frequency reduces with an increase in ε_{rod}. It is also depicted that for a fixed ε_{rod}, center frequency reduces with an increase in d/a ratio. However, for lower ε_{rod}, we do not observe much difference in center frequency with a change in d/a ratio. It is also evident that the slope of curves increases with an increase in d/a ratio which means that tuning

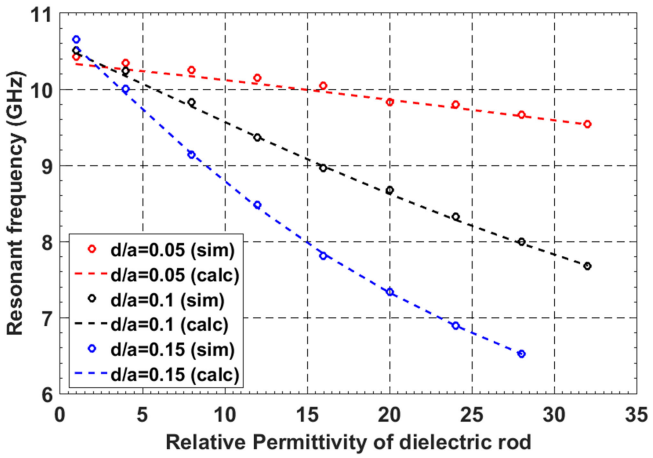

FIGURE 15. Variation of center frequency of SIW BPF with respect to relative permittivity for different diameter of dielectric rods.

of resonant frequency is more sensitive to the higher ratio of d/a. The analysis is done considering all dielectric rods lossless.

So, from the above analysis, the center frequency of the SIW BPF gets tuned due to a change in permittivity of dielectric rods present at the center of the resonant cavities only. Since the center frequency gets changed, the fractional bandwidth of the BPF also gets changed due to fixed dimensions of the iris windows. To maintain a fixed fractional bandwidth for different tuned center frequencies, iris windows must be tuned simultaneously which is analyzed in the next part.

3) ANALYSIS TO MAINTAIN CONSTANT BANDWIDTH WITH CHANGE IN CENTER FREQUENCY OF THE PROPOSED BPF

According to the conventional design procedure of iris window coupled BPF, the dimensions of the iris windows are fixed for a given center frequency and BW of the BPF as described in [50]. As the center frequency of the BPF is tuned, the K-inverter values corresponding to the iris windows also get changed which does not maintain constant bandwidth. For a given bandwidth, the required K-inverter values should be calculated for the complete band of operation according to [50]. For example, the required values of K-inverters for a third order BPF with 0.3 GHz bandwidth in X-band are plotted in Fig. 16(a) and (b), shown in dashed lines.

The K-inverter values of an iris window can be varied by putting a dielectric rod at its center and changing its relative permittivity. An iris window with a dielectric rod inside SIW is simulated and its K-inverter value is calculated from its S-parameters. Fig. 16(a) and (b) show that the required values of ε_{rod} are obtained from the intersection of simulated K-inverter curves (represented by solid lines) with the calculated ideal K-inverter curves (represented by dashed lines) for K_{01} and K_{12}. So, to meet the required K_{01} values at the center frequency of 9, 10 and 11 GHz, ε_{rod} must be chosen as 15.9, 10.2 and 6 respectively as depicted in Fig. 16(a). Similarly,

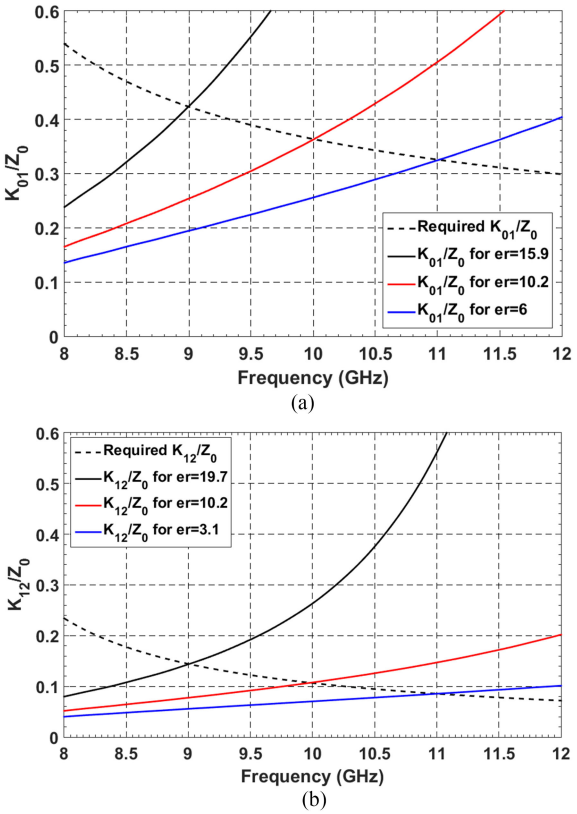

FIGURE 16. Variation of (a) K_{01}/Z_0 and (b) K_{12}/Z_0 values for 0.3 GHz bandwidth for center frequency of 9, 10, and 11 GHz.

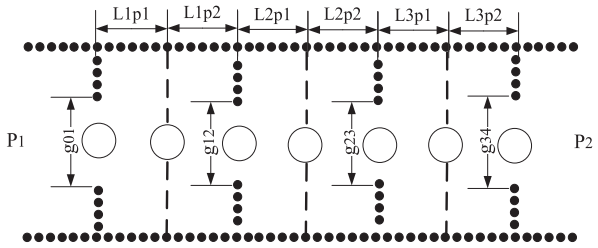

FIGURE 17. Layout of the reconfigurable SIW BPF with constant bandwidth.

from Fig. 16(b) for K_{12}, the respective values of ε_{rod} will be 19.7, 10.2 and 3.1.

So, the steps to design a reconfigurable SIW BPF with constant bandwidth are as follows. First, the ε_{rod} value of dielectric rods in the iris windows are obtained as described above. The corresponding image phase is also calculated. Then using these image phase values and the physical lengths of the cavities, ε_{rod} value of dielectric rods at the center of the cavities are determined from (7)–(9). The corresponding layout of this reconfigurable SIW BPF is shown in Fig. 17, where dielectric rods are placed at the center of cavities as well as apertures.

The proposed technique is summarized in Fig. 18 according to different design requirements. The flow chart depicts two tuning approaches to be followed to satisfy different tuning specifications. The flow chart starts with the design criteria of a filter and then checks whether the bandwidth of the reconfigurable filter needs to be maintained or not. Depending on the condition, it follows either the simple and straightforward on-field tuning, or the wide band tuning technique that requires proper calculation and look up table. The flow chart describes the complete design process in a step-by-step manner as shown in the next page. Once the desired response is achieved the design process completes otherwise it goes back to tuning stage and repeats the steps.

For example, a reconfigurable BPF is to be designed, for the given specification of a 3rd order Chebyshev type SIW iris window BPF at 10 GHz with 300 MHz bandwidth, following two different approaches of the flow chart, to tune the center frequency depending on the bandwidth requirement.

The first approach follows the steps of simple on-field reconfigurable BPF. First, a filter is designed with air holes at the center of the cavities only or at both cavities and apertures. Then to tune it to a lower frequency, dielectric rods of higher ε_{rod} value (e.g., 10.2) are initially inserted in the cavities/apertures. If the desired tuned frequency is not achieved, then the center frequency is further tuned to a lower or higher frequency in the next step to achieve the target center frequency. If the desired frequency is lower than the achieved frequency, then dielectric rods of higher values of ε_{rod} (e.g., 37) are inserted. On the other hand, if the desired frequency is higher than the achieved frequency, then dielectric rods of lower values of ε_{rod} (e.g., 2.2) are inserted. Once the desired frequency response is achieved, the design process is completed.

The second approach follows the steps to design wide band reconfigurable BPF while maintaining constant bandwidth. In the first step, the filter is designed with dielectric rods of $\varepsilon_{rod} = 10.2$ at the center of cavities and apertures. In the next step, the required values of the relative permittivities of the rods are calculated to make the look up table for center frequency tuning while keeping the bandwidth of the filter unchanged. Then the required set of dielectric rods are inserted according to the calculated lookup table, to complete the design process.

III. RESULTS AND DISCUSSIONS

A. SIMPLE ON-FIELD RECONFIGURABLE SIW BPF

Reconfigurable SIW BPFs are designed and fabricated on Rogers 5880B substrate of relative permittivity 2.2 and height of 0.508 mm. Then dielectric rods of different dielectric materials are fabricated from respective materials separately. For $\varepsilon_{rod} = 2.2$, tan δ=0.0009 and ε_{rod} =10.2, tan δ=0.0023 rods are fabricated from two soft substrates Rogers 5880B and Rogers 6010 by using Laser cutting. Then ceramic material is grinded to fabricate rods of $\varepsilon_{rod} = 37$, tan δ=0.0005. Dielectric rods are of diameter 2 mm and height 1 mm. Due to fabrication constraints, dielectric rods (ceramic) of diameter less than 2 mm and height less than 1 mm could not be fabricated. The first measurement is done with no dielectric rods i.e., with

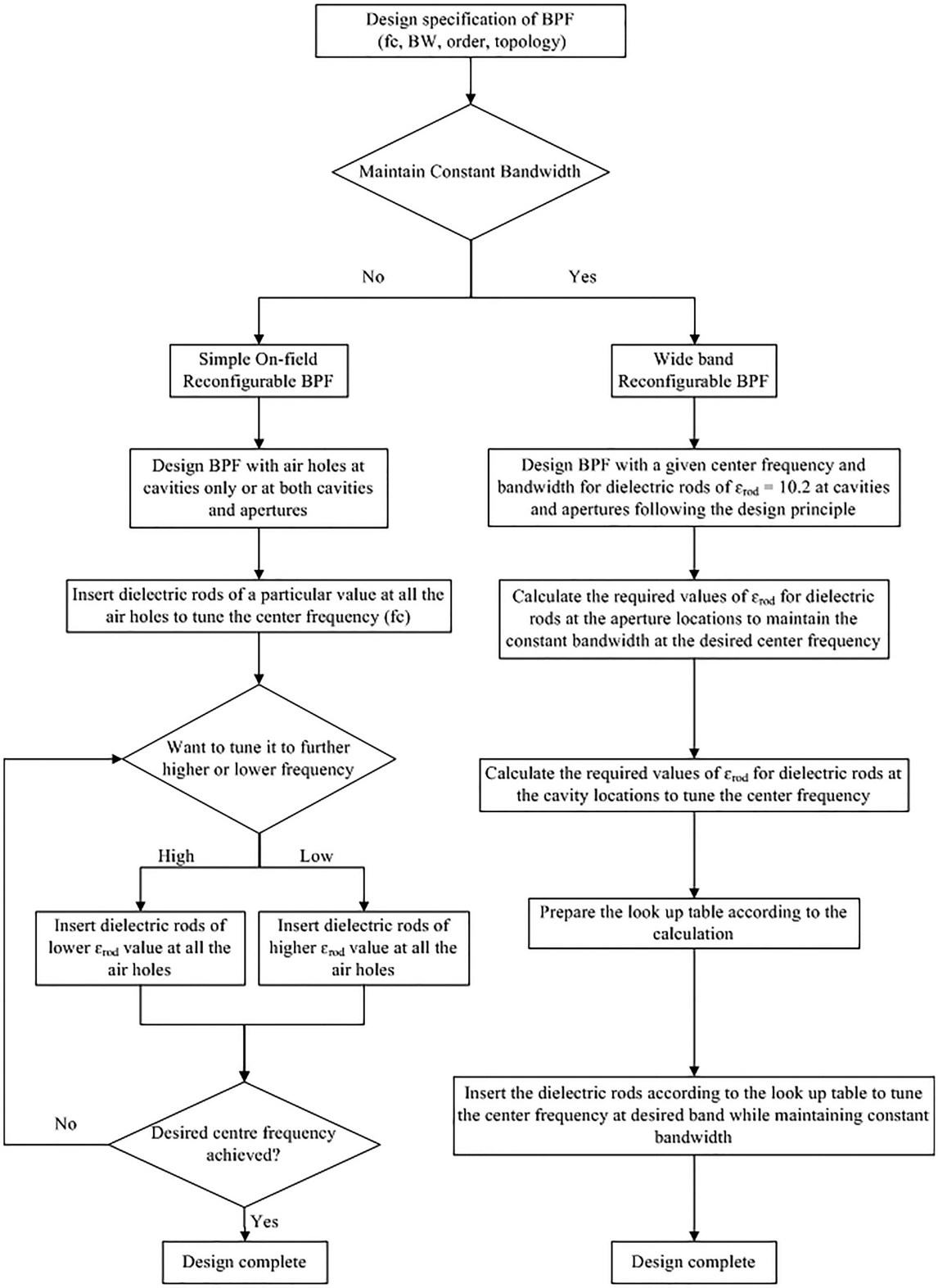

FIGURE 18. Flow chart for filter design.

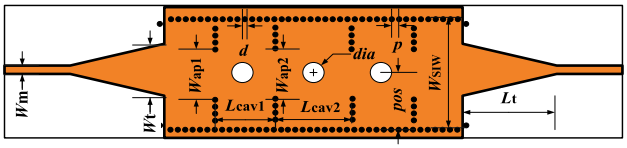

FIGURE 19. Layout of SIW iris window BPF loaded with dielectric rods at center of cavities.

TABLE 4. Geometrical Parameters of the Reconfigurable BPF [Unit: mm]

Symbol	Value	Symbol	Value
W_m	1.56	s	0.8
W_t	5.43	p	1.6
W_{SIW}	15.85	L_{cav1}	10
L_t	13.4	L_{cav2}	12
W_{ap1}	7	W_{ap2}	6.25
pos	$W_{SIW}/2$	d	2

air holes. A scotch tape is pasted at the top and bottom of the BPF, so that the rods do not misalign once they are inserted. Then dielectric rods of the same dimension and same relative permittivity (e.g., $\varepsilon_{rod} = 2.2$ for all the rods) are pressed at all the air holes to perform the next measurement. Similarly, four sets of measurements are done corresponding to $\varepsilon_{rod} = 1$ i.e., air, then 2.2, 10.2 and 37. S-parameter response of the fabricated filters is obtained using the Agilent E8364 PNA Network analyzer. In most of the cases, the measured and simulated results agree well.

1) DIELECTRIC RODS IN CAVITIES ONLY

To show center frequency tunability, the first position of dielectric rods is chosen at the center of the cavities only as shown in Fig. 19 and then ε_{rod} is varied. Initially, ε_{rod} is chosen as 1, which means air holes only at the center of cavities. Then their diameter 'd' is optimized simultaneously for all air holes and the best response is obtained for 'd' = 2 mm. The critical geometrical parameters after optimization of the designed reconfigurable SIW BPF are given in Table 4.

Then their relative permittivity is varied starting from that of the substrate itself i.e., 2.2, then 10.2 and 37. In this type of arrangement, the effect of rods can be seen in the electric field pattern inside the filter. The magnitude of the electric field at the center frequency of 10.9 GHz for $\varepsilon_{rod} = 37$, is shown in Fig. 20.

It can be observed that all the three resonant cavities are resonating at similar frequencies. Identical field patterns have been observed for other dielectric rods as well. Dielectric rods allow an electric field to propagate through them. Whereas metallic screws reflect electric field from their surface. So dielectric rods cause minimum field perturbation in comparison to metallic tuning screws, and hence better insertion loss and return loss can be achieved over a wide bandwidth.

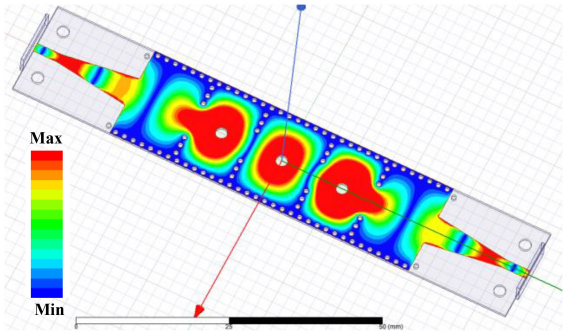

FIGURE 20. Simulated electric field pattern at center frequency of 10.9 GHz with loaded dielectric rods of $\varepsilon_{rod} = 37$.

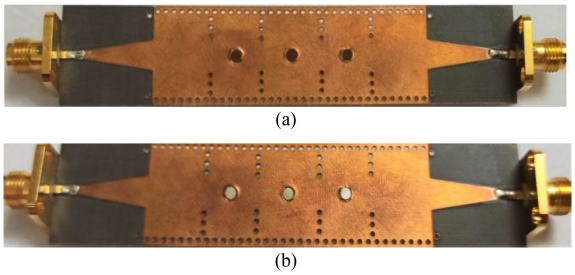

FIGURE 21. Photograph of reconfigurable SIW bandpass filter (a) without and (b) with dielectric rods at the center of the cavities only (dimension: 90 mm × 18 mm).

For the measurement purpose, dielectric rods of different dielectric materials are loaded one by one, into the air holes in the cavities of SIW BPF as shown in Fig. 21. Initially, the filter with air holes is measured. Then dielectric rods are pressed into air holes with permittivity equal to 2.2 (i.e., Rogers 5880 rods), 10.2 (i.e., Rogers 6010 rods), and then 37 (i.e., ceramic rods), one by one. Thus, four sets of measurements are taken.

Fig. 22(a) shows simulated and measured S_{11} of the designed filter where it is observed that center frequency of the filter is tuned to lower frequency as permittivity of dielectric rods increases. Center frequency of this SIW BPF is tuned from 10.8 GHz (for air case) to 11.5 GHz (for $\varepsilon_{rod} = 37$ case) as depicted in Fig. 22(b). Total tunability of 700 MHz is achieved in center frequency using this much variation in relative permittivity of dielectric rods from $\varepsilon_{rod} = 1$ to $\varepsilon_{rod} = 37$. So center frequency tunability up to 6.3% is observed using this simple mechanical tuning with dielectric rods at the center of cavities [51]. Extracted unloaded Q-factor from the measurements varies in the range of 101.97-122.8 along with tuning.

2) DIELECTRIC RODS IN CAVITY AND APERTURE

To maintain constant bandwidth with center frequency tunability, dielectric rods are placed both at the center of the apertures and cavities and their permittivity is varied [51]. In contrast to the previous filter, tuning rods are changing the resonant frequency of each resonator along with the K-inverter values associated with the coupling windows between resonators. Here also their diameter 'd' is set at 2 mm as

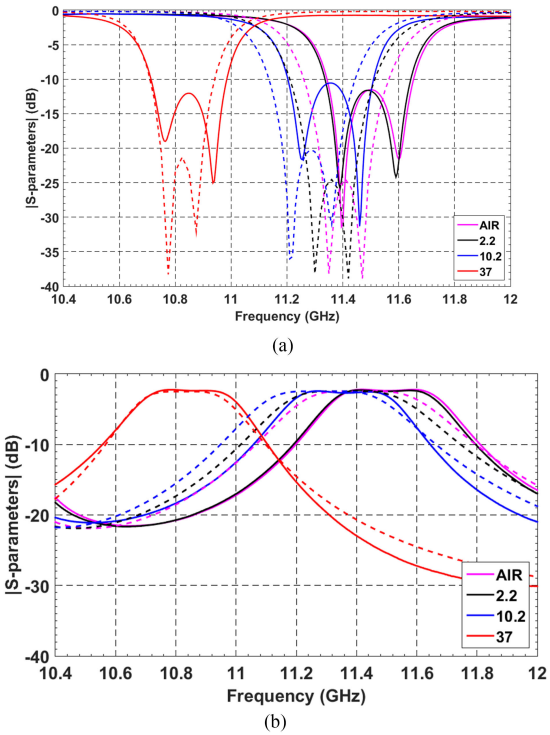

FIGURE 22. Simulated (dotted lines) and measured (solid lines) (a) return loss and (b) insertion loss of Fig. 19 with the change in the dielectric material of dielectric rods.

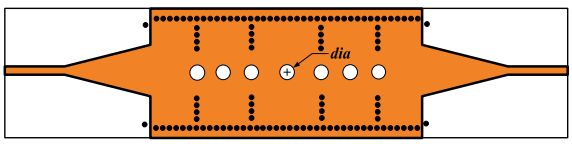

FIGURE 23. Layout of SIW iris window BPF loaded with dielectric rods at the center of cavity and aperture.

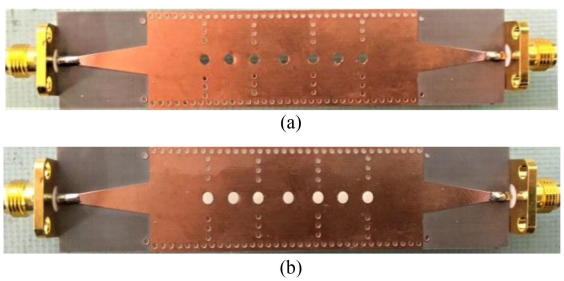

FIGURE 24. Photograph of reconfigurable SIW bandpass filter (a) without and (b) with dielectric rods at the center of cavities and apertures (dimension: 90 mm × 18 mm).

shown in Fig. 23. Dimensions of this design are the same as that of the previous one, as depicted in Table 3, with the only exception in the location of dielectric rods. In the simulation, the permittivity of the rods is varied starting from 1 to that of the substrate itself i.e., 2.2, then 10.2 and 37. The fabricated circuit is shown in Fig. 24. Initially, the filter with air holes is measured. Then dielectric rods with relative permittivity equal to 2.2, 10.2 and 37 are pressed into those air holes one by one

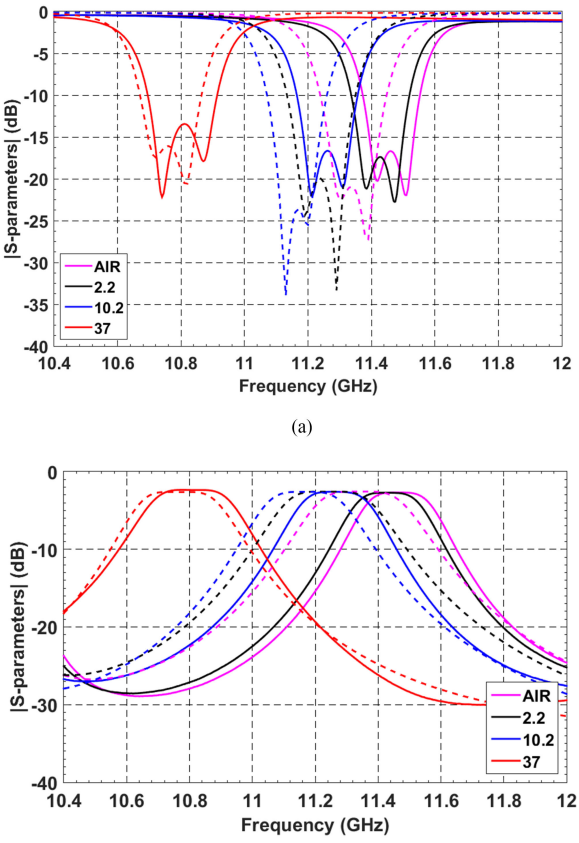

FIGURE 25. Simulated (dotted lines) and measured (solid lines) (a) Return loss and (b) Insertion loss of SIW BPF shown in Fig. 23 with change in permittivity of dielectric rods.

and three more sets of measurements are taken. As shown in Fig. 25, it is observed in the measured results that for air case, fc is at around 11.45 GHz, which is tuned to approximately 10.85 GHz for that of $\varepsilon_{rod} = 37$ case. So, the total center frequency tuning range of almost 600 MHz is obtained, by maintaining constant bandwidth for each case. The range of extracted unloaded Q-factor is 139.1-210.5.

From the measurements of the above cases, it is observed that the center frequency tunability is dependent on the placement of the dielectric rods in the BPF. For a given physical length of the cavity, the corresponding electrical length can be varied more, by placing dielectric rods in the cavities only. Hence this gives more tunability of center frequency. In comparison to the other case, it is easier to operate the BPF in this configuration since it requires a smaller number of dielectric rods. Hence this configuration is preferred to obtain easy tunability, like for on-field or on-tower tunning and performance optimization However, for less cost sensitive applications, for maintaining constant bandwidth with good central frequency tuning, the second configuration is proposed and detailed as below. Here the required relative permittivities are calculated according to the K-inverter values and took up table is required to be followed for reconfiguring BPF using dielectric rods.

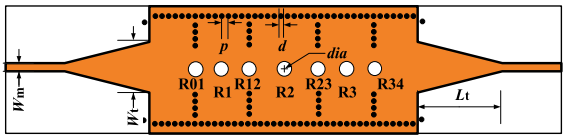

FIGURE 26. Layout of SIW iris window BPF loaded with dielectric rods.

TABLE 5. Geometrical Parameters of the Reconfigurable BPF [Unit: mm]

Symbol	Value	Symbol	Value
W_m	1.56	s	0.8
W_t	5.43	p	1.6
Lt	13.4	d	2
L1p1	4.3	g01	7
L2p1	5.1	g12	4.84
L3p1	4.3	g23	4.84
L1p2	4.3	g34	7
L2p2	5.1	L3p2	4.3

TABLE 6. Lookup Table of Dielectric Rods

	f_c in GHz	R_1	R_2	R_3	R_{01}	R_{12}	R_{23}	R_{34}
Case1	10	10.2	10.2	10.2	10.2	10.2	10.2	10.2
Case2	10.5	8.5	8	8.5	8	6.5	6.5	8
Case3	11	7.1	6	7.1	6	3.1	3.1	6
Case4	11.97	4.4	2.2	4.4	4.4	2.2	2.2	4.4

B. WIDE BAND RECONFIGURABLE BPF WITH CONSTANT BW

The second configuration from the last section is considered for further analysis. Dielectric rods for tuning of each resonator (R1, R2 and R3), for coupling between each pair of resonators (R12 and R23) and for input/output signal coupling (R01 and R34) are placed as shown in Fig. 26. At first, ε_{rod} of R_{01}, R_{12}, R_{23} and R_{34} are chosen as 10.2 since this is very easily available for simple and inexpensive in-house machining. Then using image phase and physical length of the BPF, ε_{rod} of R_1, R_2 and R_3 are calculated to design the BPF at 10 GHz. This is considered as case 1 where ε_{rod} of all the rods are 10.2. The critical geometrical parameters after optimization of the designed BPF from Fig. 17 and 26 are given in Table 5. Then, ε_{rod} of R_1, R_2 and R_3 are changed to show center frequency tunability. To maintain the constant bandwidth at the different center frequencies, required values of K-inverters are different. These values are determined by ε_{rod} of R_{01}, R_{12}, R_{23} and R34. So, these values are calculated accordingly. Three other different combinations of ε_{rod} are given in the form of a look up table in Table 6, which tunes the complete filter response at three different center frequencies, maintaining the constant filter bandwidth. The designed SIW BPF is

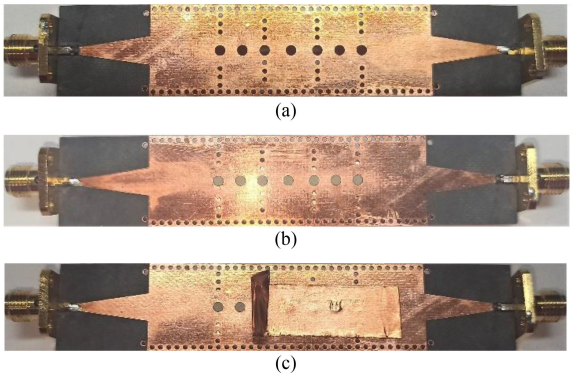

FIGURE 27. Photograph of reconfigurable SIW BPF (a) without dielectric rods, (b) with rods, and (c) showing top view with rods partially covered with copper tape (dimension: 90 mm × 18 mm).

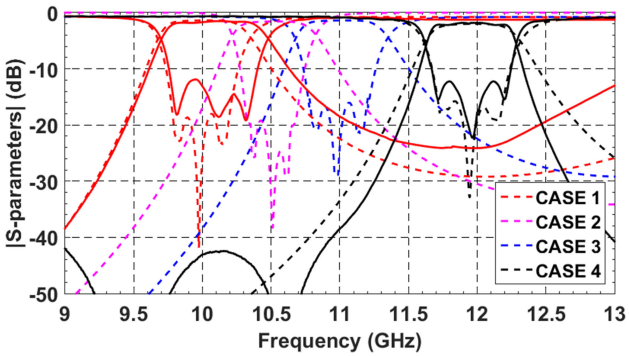

FIGURE 28. Simulated (dotted lines) and measured (solid lines) S-parameter response of SIW BPF with the change in the dielectric material of dielectric rods.

fabricated, and dielectric rods of different dielectric materials are fabricated from respective materials separately. For ε_{rod} = 2.2, tan δ=0.0009, ε_{rod} =10.2, tan δ=0.0023 and ε_{rod} = 4.4, tan δ=0.02 rods are fabricated from three substrates viz. Rogers 5880B, Rogers 6010 and FR4 by using Laser cutting. Since the combination of cases 1 and 4 are quite easily available in the laboratory, only these two cases are considered for measurement. Dielectric rods are of diameter 2 mm and height 0.732 mm. For measurement, dielectric rods are loaded into the air holes in the cavities and apertures of SIW BPF as shown in Fig. 27. The first measurement is done with 10.2 rods for case 1. After inserting the rods, the copper tape is pasted at the top and bottom of the BPF, so that the rods do not misalign once they are inserted, and it also reduces the radiation loss. S-parameter response of the fabricated filter is obtained using the Agilent E8364 PNA.

Similarly, the next measurement is done after loading the next set of dielectric rods (ε_{rod} =4.4 and 2.2). Fig. 28 shows the simulated and measured frequency response of the designed filter. Center frequency of the BPF is tuned from 10.1 GHz (case 1) to 11.97 GHz (case 4) as depicted in measured results. Total tunability of 1.87 GHz i.e., 16.9% is achieved in center frequency while maintaining constant bandwidth. Extracted unloaded Q-factor from the measurements varies in the range of 81.15-98.94 along with tuning. Thus,

TABLE 7. Figure of Merit Comparison of Existing Tunable SIW Filters

Technique	Order of the filter	CF (GHz)	FBW (%)	Advantage/ Disadvan-tage	IL (dB)
PIN Diode [11]	2	4.2	1.5-2	External DC bias Parasitics	3
PIN Diode [31]	2	1.8	2.3-3	External DC bias Parasitics	4.5
MEMS based [32]	2	1.4	3.2-4.2	External DC bias Parasitics	3.2-8.8
Varactor diode [33]	1	10.5	NA	External DC bias Parasitics	NA
Ferro-electric [34]	2	3.26	5.4	External DC bias Parasitics	2.6-3.3
Varactor and Ferrite [36]	2	12	4.2-4.7	External DC bias Parasitics	2-5
Switch-able capacitive post [38]	1	10	1.06	No DC bias Difficult to adjust active-tion lead	1.9-2.1
Metallic screws and flaps [39]	4	10	6.3	No DC bias Difficult to integrate	4-5
Mecha-nical flaps [40]	2	7.5	2-4.6	No DC bias Difficult to adjust flap angle	1.3
Radially moving copper column [41]	2	13.82	2.9-5.98	Mobile copper column causes erosion with time	1.7-2.8
Proposed technique	**3**	**11.1** **11.0**	**1.78-3.5** **5.3-7.6**	**No DC bias Easy to integrate**	**1.5-1.8**

CF: Center Frequency, FBW: Fractional Bandwidth, IL: Insertion Loss

wideband reconfigurable BPF can be designed using the proposed technique. Although this technique is a bit complex in terms of calculation and lookup table follow up in the practical scenario. But this gives more accurate results (in terms of BW and rejection). For easier and much simpler tuning, including for applications like on field tunning, the first approach is more suitable, and no lookup table is required.

The performance of the proposed passive tuning technique is compared with other previously reported active and passive tuning techniques in Table 7.

As shown in the state-of-art table, the proposed tuning technique is low profile and cost-effective. The technique removes the requirement of additional DC bias circuitry which makes active tuning complex [11], [31]–[36] reduces reliability, and increases cost and power consumption. This technique also makes the cost of CPE (in a hard-to-reach area) more affordable. The designed filter can be scaled for any desired frequency of operation by simply altering its dimension. This removes frequency limitation which is the main constraint for active tuning where varactor diodes are used. Also, in the Q-factor analysis (Section II and Table 2), it is shown that the dielectric rods have a higher Q-factor in comparison to that of the metallic structures, and hence dielectric rods are less lossy than metallic screws, or flaps which are mostly used in conventional passive tuning techniques. As a result, above 10 GHz, the proposed technique demonstrates lowest loss performance and higher bandwidth, compared to widely used metal screw, flap or column based passive techniques [38]–[41] ever reported.

This technique can be extended further for remote-control and faster tuning applications. The insertion of the rod with a stack of different dielectric materials as a screw can be controlled mechanically with a motor. For industrial application, as an alternative to pasting the copper tapes, dielectric rods with metal coating on the top and bottom sides can be used. Further, for applications like CPEs of a P2MP and P2P radios, where TRX filters operates at pre-decided fixed frequency bands, as an alternative to copper tape a metal layer can be printed (using a portable 3D printer).

The air holes are drilled with a smaller diameter than that of the dielectric rods, so that the rods can be fit into them tightly. Since the dielectric rods are machined from commonly available substrates, they can be very easily pressed inside the air holes that are drilled in Rogers 5880, which is very soft substrate.

The overall tuning technique is also suitable for temperature compensation, where the performance deviation with temperature plays a critical role, such as in high-power transmitters/base station applications. Dielectric materials with opposite/different temperature coefficients, such as Barium Magnesium Tantalite (BMT), can be used for temperature compensation.

IV. CONCLUSION

In this paper, a simple mechanically tuning technique for realizing low profile reconfigurable filters using dielectric rods, manufactured from commonly used dielectric substrates, is presented with detailed theoretical analysis and experimental results. The proposed technique has been developed for industrial applications (including for high speed, long distance fixed wireless connectivity in a remote area), where keeping the fabricated physical structure of the BPF same, the frequency can be reconfigured for optimum performance and matching with the required channel or band of a multichannel or multi-band wireless module. First, a straightforward technique is proposed, for low-profile on field applications, where permittivity of all the dielectric rods inside BPF is changed simultaneously without any calculation or look up table. In this technique, all the dielectric rods are replaced simultaneously with another set of rods of the same but different (higher) dielectric constant, for moving the center frequency of the band to other (lower) frequency. This enables very easy and convenient on-field/on tower type applications for a point to point/multipoint radio. Whereas the second technique illustrates better performance (in terms of wider and constant BW and better rejection) at the cost of a lookup table and a relatively wider range of permittivities of dielectric rods, which makes the process bit complex and expensive. The

proposed technique is simple and cost-effective in comparison to other available active tuning techniques since it removes the use of complex DC bias circuitry and makes the system more reliable. Moreover, as demonstrated with measured results and shown in performance comparison table, the reconfigurable SIW filters achieved higher-Q and hence lowest insertion loss (1.5–1.8 dB) at high frequencies (>10 GHz), yet higher FBW, compared to reported tuning techniques, including passive tunning techniques using metallic flap, screw, or column. Further, this technique can be used for compensating performance deviation and optimizing performance due to manufacturing uncertainties and for temperature compensation of a compact wireless front-end module.

REFERENCES

[1] K. K. Samanta, D. Stephens, and I. D. Robertson, "Design and development of a 60 GHz multi-chip module receiver employing substrate integrated waveguides," *IET Microw. Antennas Propag.*, vol. 1, no. 5, pp. 961–996, Oct. 2007.

[2] I. C. Hunter and J. D. Rhodes, "Electronically tunable microwave band-pass filters," *IEEE Trans. Microw. Theory Techn.*, vol. 30, no. 9, pp. 1354–1360, Sep. 1982.

[3] M. Makimoto and M. Sagawa, "Varactor tuned band-pass filters using microstrip-line ring resonators," in *IEEE MTT-S Int. Microw. Symp. Dig.*, 1986, pp. 411–414.

[4] C. Musoll-Anguiano, I. Llamas-Garro, Z. Brito-Brito, L. Pradell, and A. Corona-Chavez, "Fully adaptable band-stop filter using varactor diode," *IEEE Microw. Wireless Compon. Lett.*, vol. 52, no. 3, pp. 554–558, 2002.

[5] G. A. Swartz, D. W. Wern, and P. H. Robinson, "Large-area varactor diode for electrically tunable, high-power UHF band-pass filter," *IEEE Trans. Electron. Devices*, vol. 27, no. 11, pp. 2146–2151, Nov. 1980.

[6] F. L. Yu, X. Y. Zhang, and Y. B. Zhang, "Frequency-tunable band-pass filters with constant absolute bandwidth and improved linearity," *Prog. Electromagnetics Res. Lett.*, vol. 33, pp. 131–140, 2012.

[7] S. Sam and S. Lim, "Frequency reconfigurable substrate integrated waveguide antenna," in *Proc. IEEE ISAP*, 2012, pp. 822–825.

[8] C. Lugo and J. Papapolymerou, "Electronic switchable band-pass filter using PIN diodes for wireless low cost system-on-a-package applications," *IET Microw. Antennas Propag.*, vol. 151, no. 6, pp. 497–502, Dec. 2004.

[9] Z. Brito-Brito, I. Llamas-Garro, L. Pradella-Cara, and A. Corona-Chavez, "Microstrip switchable bandstop filter using PIN diodes with precise frequency and bandwidth control," in *Proc. Eur. Microw. Week*, 2008, pp. 1707–1711.

[10] M. F. Karim, Y.-X. Guo, Z. N. Chen, and L. C. Ong, "Miniaturized reconfigurable and switchable filter from UWB to 2.4 GHz WLAN using PIN diodes," in *IEEE MTT-S Int. Microw. Symp. Dig.*, 2009, pp. 509–512.

[11] S. Sirci, J. D. Martinez, and V. E. Boria, "Low-loss 3-bit tunable SIW filter with PIN diodes and integrated bias network," in *Proc. Eur. Microw. Conf.*, 2013, pp. 1211–1214.

[12] H. Jiang, B. Lacroix, K. Choi, Y. Wang, A. T. Hunt, and J. Papapolymerou, "A compact ferroelectric tunable band-pass filter with flexible frequency responses," in *Proc. IEEE Int. Conf. Wireless Inf. Technol. Syst.*, 2012, pp. 1–4.

[13] C. E. Fay, "Ferrite tuned resonant cavities," *Proc. IRE*, vol. 44, pp. 1446–1449, 1956.

[14] P. S. Carter, "Magnetically-tunable microwave filters using single-crystal yttrium-irongarnet resonators," *IRE Trans. Microw. Theory Techn.*, vol. 9, pp. 252–260, 1961.

[15] Y. Murakami, T. Ohgihara, and T. Okamoto, "A 0.5-4-GHz tunable band-pass filter using YIG film grown by LPE," *IEEE Trans. Microw. Theory Techn.*, vol. 35, pp. 1192–1198, Dec., 1987.

[16] A. S. Tatarenko, V. Gheevarughese, and G. Srinivasan, "Magnetoelectric microwave band-pass filter," *Electron. Lett.*, vol. 42, pp. 540–541, Dec. 2006.

[17] C. S. Tai and G. Qiu, "Wideband microwave filters using ferromagnetic resonance tuning in flip-chip YIG-GaAs layer structures," *IEEE Trans. Magn.*, vol. 45, no. 2, pp. 656–660, Feb. 2009.

[18] X. Y. Zhang, C. H. Chan, Q. Xue, and B.-J. Hu, "RF tunable band stop filters with constant bandwidth on a doublet configuration," *IEEE Trans. Microw. Theory Techn.*, vol. 59, no. 2, pp. 1257–1265, Feb. 2012.

[19] M. Ouaddari, S. Delprat, F. C. Vidal, M. Chaker, and K. Wu, "Microwave characterization of ferroelectric thin-film materials," *IEEE Trans. Microw. Theory Techn.*, vol. 53, no. 4, pp. 1390–1397, Apr. 2005.

[20] J. Papapolymerou, C. Lugo, Z. Zhiyong, and X. Wang, "A miniature low-loss slowwave tunable ferroelectric band-pass filter from 11–14 GHz," in *IEEE MTT-S Int. Microw. Symp. Dig.*, 2006, pp. 556–559.

[21] S. L. Delprat, C. Durand, J. Oh, M. Chaker, and K. Wu, "Correlation between the lattice parameter and the dielectric tunability in nonepitaxial Ba0.5Sr0.5TiO3 thin films," *Appl. Phys. Lett.*, vol. 91, pp. 063513–063513–3, 2007.

[22] E. Lourandakis, M. Schmidt, G. Fischer, and R. Weigel, "A ferroelectric tunable combline filter with improved stopband transitions," in *Proc. IEEE Radio Wireless Symp.*, 2009, pp. 340–343.

[23] S. Courreges, Y. Li, Z. Zhao, K. Choi, A. T. Hunt, and J. Papapolymerou, "Two-pole X-band-tunable ferroelectric filters with tunable center frequency, fractional bandwidth and return loss," *IEEE Trans. Microw. Theory Techn.*, vol. 57, no. 12, pp. 2872–2881, Dec. 2009.

[24] L. Pantoli, V. Stornelli, and G. Leuzzi, "A single-transistor tunable filter for bluetooth applications," in *Proc. Eur. Microw. Integr. Circuits Conf.*, 2012, pp. 889–892.

[25] A. Ocera, P. Farinelli, P. Mezzanotte, R. Sorrentino, B. Margesin, and F. Gaicomozzi, "A novel MEMS-tunable hairpin line filter on silicon substrate," in *Proc. Eur. Microw. Conf.*, 2006, pp. 803–806.

[26] K. Y. Chan, S. Fouladi, R. Ramer, and R. R. Mansour, "MEMS switchable interdigital band-pass filter," *IEEE Microw. Wireless Compon. Lett.*, vol. 22, no. 1, pp. 44–46, Jan. 2012.

[27] W. Gautier, A. Stehle, B. Schoenlinner, V. Ziegler, U. Prechtel, and W. Menzel, "RF-MEMS tunable filters on low-loss LTCC substrate for UAV data-link," in *Proc. Eur. Microw. Integr. Circuits Conf. (EuMIC)*, 2009, pp. 347–350.

[28] J.-H. Park, S. Lee, J.-M. Kim, H.-T. Kim, Y. Kwon, and Y.-K. Kim, "Reconfigurable millimeter-wave filters using CPW-based periodic structures with novel multiple-contact MEMS switches," *J. Microelectromech. Syst.*, vol. 14, no. 3, pp. 556–563, 2005.

[29] E. Fourm *et al.*, "Bandwidth and central frequency control on tunable band-pass filter by using MEMS cantilevers," in *IEEE MTT-S Int. Microw. Symp. Dig.*, vol. 1, 2003, pp. 523–526.

[30] M. Bozzi, A. Georgiadis, and K. Wu, "Review of substrate-integrated waveguide circuits and antennas," *IET Microw. Antennas Propag.*, vol. 5, no. 8, pp. 909–920, 2011.

[31] M. Armendariz, V. Sekar, and K. Entesari, "Tunable SIW bandpass filters with PIN diodes," in *Proc. 40th Eur. Microw. Conf.*, Sep. 2010, pp. 830–833.

[32] V. Sekar, M. Armendariz, and K. Entesari, "A 1.2–1.6 GHz substrate-integrated waveguide RF MEMS tunable filter," *IEEE Trans. Microw. Theory Techn.*, vol. 59, no. 4, pp. 866–876, Apr. 2011.

[33] F. He, K. Wu, and H. Wei, "Electrically tunable half mode substrate integrated waveguide resonator," in *Proc. Asia-Pacific Microw. Conf.*, 2011, pp. 1166–1169.

[34] Y. L. Zheng, M. Sazegar, and H. Maune, "Compact substrate integrated waveguide tunable filter based on ferroelectric ceramics," *IEEE Microw. Wireless Compon. Lett.*, vol. 21, no. 9, pp. 477–479, Sep. 2011.

[35] M. Almalkawi, L. Zhu, and V. Devabhaktuni, "Magnetically tunable substrate integrated waveguide bandpass filters employing ferrites," in *Proc. 36th Int. Infrared, Millimeter, THz Waves Conf.*, Oct. 2011, pp. 1–2.

[36] S. Adhikari, A. Ghiotto, and K. Wu, "Simultaneous electric and magnetic two-dimensionally tuned parameter-agile SIW devices," *IEEE Trans. Microw. Theory Techn.*, vol. 61, no. 1, pp. 423–435, Jan. 2013.

[37] A. Djermoun, G. Prigent, N. Raveu, and T. Callegari, "Widely tunable high-Q SIW filter using plasma material," in *IEEE MTT-S Int. Dig.*, May 2010, pp. 1484–1486.

[38] J. C. Bohorquez *et al.*, "Reconfigurable planar SIW cavity resonator and filter," in *IEEE MTT-S Int. Dig.*, Jun. 2006, pp. 947–950.

[39] F. Mira, J. Mateu, and C. Collado, "Mechanical tuning of substrate integrated waveguide filters," *IEEE Trans. Microw. Theory Techn.*, vol. 63, no. 12, pp. 3939–3946, Dec. 2015.

[40] H. Zhang, W. Kan, and W. Wu, "Balanced bandpass filter with tunable centre frequency based on substrate integrated waveguide technology," *Electron. Lett.*, vol. 54, no. 14, pp. 886–888, Jul. 2018.

[41] F. Huang, J. Zhou, and W. Hong, "Ku band continuously tunable circular cavity SIW filter with one parameter," *IEEE Microw. Wireless Compon. Lett.*, vol. 26, no. 4, pp. 270–272, Apr. 2016.
[42] J. H. Dang, R. C. Gough, A. M. Morishita, A. T. Ohta, and W. A. Shiroma, "A tunable x-band substrate integrated waveguide cavity filter using reconfigurable liquid-metal perturbing posts," in *Proc. IEEE MTT-S Int. Microw. Symp.*, Phoenix, AZ, 2015, pp. 1–4.
[43] Y. Kobayashi and S. Yoshida, "Bandpass filters using dielectric rod resonators," in *IEEE MTT-S Int. Dig.*, vol. 78, no. 1, pp. 233–235, Jun. 1978.
[44] D. D. Zhang, L. Zhou, L. S. Wu, L. F. Qiu, W. Y. Yin, and J. F. Mao, "Novel bandpass filters by using cavity-loaded dielectric resonators in a substrate integrated waveguide," *IEEE Trans. Microw. Theory Techn.*, vol. 62, no. 5, pp. 1173–1182, May 2014.
[45] L. Wu, L. Zhou, X. Zhou, and W. Yin, "Bandpass filter using substrate integrated waveguide cavity loaded with dielectric rod," *IEEE Microw. Wireless Compon. Lett.*, vol. 19, no. 8, pp. 491–493, Aug. 2009.
[46] S. De, S. K. Koul, and K. K. Samanta, "Tunable substrate integrated waveguide filters," in *Proc. IEEE- MTT Int. Microw. Radio Conf.*, Mumbai, India, Dec. 2019.
[47] Y. Cassivi and K. Wu, "Low cost microwave oscillator using substrate integrated waveguide cavity," *IEEE Microw. Wireless Compon. Lett.*, vol. 13, no. 2, pp. 48–50, Feb. 2003.
[48] N. Marcuvitz, *Waveguide Handbook*. New York, NY, USA: McGraw Hill Book Company, Inc., 1951, pp. 221–267.
[49] D. M. Pozar, *Microwave Engineering*, 4th ed. New York, NY, USA: Wiley, 2012.
[50] G. L. Matthaei, L. Young, and E. M. T. Jones, *Microwave Filters, in Impedance-Matching Networks and Coupling Structures*. Norwood, MA, USA: Artech House, 1980, pp. 436–458.
[51] K. K. Samanta, S. De, and S. K. Koul, "Tunable substrate integrated waveguide filters," Indian Patent Application No: 201911030536, Jul. 29, 2019.

SRIPARNA DE (Graduate Student Member, IEEE) received the B.Tech. degree in electronics and communication engineering from the West Bengal University of Technology, Kolkata, India, in 2014, and the M.Tech. degree in electronics and telecommunication engineering from Jadavpur University, Kolkata, India, in 2016. She is currently working toward the Ph.D. degree with the Indian Institute of Technology Delhi, New Delhi, India. She is currently with the Centre for Applied Research in Electronics (CARE), Indian Institute of Technology Delhi. Her research interests include substrate integrated waveguide circuits for microwave and millimeter-wave applications.

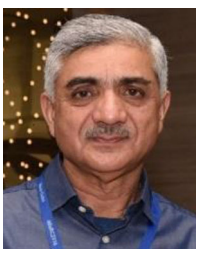

SHIBAN K. KOUL (Life Fellow, IEEE) received the B.E. degree in electrical engineering from Regional Engineering College, Srinagar, India, in 1977, and the M.Tech. and Ph.D. degrees in microwave engineering from the Indian Institute of Technology Delhi (IIT Delhi), New Delhi, India, in 1979 and 1983, respectively.

He has been an Emeritus Professor with IIT Delhi, since 2019 and the Mentor Deputy Director of strategy & planning, international affairs with the Indian Institute of Technology Jammu, India, since 2018. From 2012 to 2016, he was the Deputy Director (Strategy and Planning) with IIT Delhi. He was also the Chairman of Astra Microwave Products Limited, Hyderabad, India, from 2009 to 2019 and Dr. R. P. Shenoy Astra Microwave Chair Professor with IIT Delhi from 2014 to 2019. He has successfully completed 38 main sponsored projects, 52 consultancy projects, and 61 technology development projects. He has authored or coauthored 480 research papers, 13 state-of-the-art books, four book chapters, and two e-books. He holds 16 patents, six copyrights, and one trademark. He has guided 25 Ph.D. dissertations and more than 100 master's theses. His research interests include RF MEMS, high frequency wireless communication, microwave engineering, microwave passive and active circuits, device modeling, millimeter wave IC Design, and reconfigurable microwave circuits, including antennas.

Dr. Koul is a Fellow of the Indian National Academy of Engineering, India, and the Institution of Electronics and Telecommunication Engineers (IETE), India. He is the Chief Editor of *IETE Journal of Research* and an Associate Editor for *International Journal of Microwave and Wireless Technologies*, Cambridge University Press, Cambridge, U.K. From 2012 to 2014, he was a Distinguished Microwave Lecturer of IEEE MTT-S. He is also an AdCom member of IEEE MTT-S from 2010 to 2018 and is currently a member of the awards, Nomination and Appointments, MGA, M&S, and education committees of IEEE MTT-S. He was the recipient of numerous awards, including the IEEE MTT Society Distinguished Educator Award (2014), Teaching Excellence Award (2012) from IIT Delhi, Indian National Science Academy (INSA) Young Scientist Award (1986), Top Invention Award (1991) of the National Research Development Council for his contributions to the indigenous development of ferrite phase shifter technology, VASVIK Award (1994) for the development of Ka-band components and phase shifters, Ram Lal Wadhwa Gold Medal (1995) from the Institution of Electronics and Communication Engineers (IETE), Academic Excellence Award (1998) from the Indian Government for his pioneering contributions to phase control modules for Rajendra Radar, the Shri Om Prakash Bhasin Award (2009) in the field of electronics and information technology, the VASVIK Award (2012) for the contributions made to the area of information, communication technology (ICT), and M N Saha Memorial Award (2013) from IETE.

KAMAL K. SAMANTA (Senior Member, IEEE) graduated in science (Phy Hons.) and engineering (ECE) before the double master's degree in management (R&D) and technology (ECE), and the Ph.D. degree in microwave engineering from the University of Leeds, Leeds, U.K. For more than two decades, he has been extensively involved in a wide range of industrial and government scientific research activities on advanced device/component, circuit and system design, development and packaging, covering frequency MHz to THz, and power from μW (MMICs) to Megawatts (SSPAs). He has produced many innovative and the world's first industrial solutions. His roles have included that of a Senior Principal/Lead R&D - Engineer, Scientist and Consultant. The organisations he was with include Thales Aerospace (for Radar/EW/ESM systems), European Aeronautics Defence and Space (EADS) Astrium (presently Airbus), U.K., Indian Space Research Organization (satellite payload ckts). IPR, Department of Atomic Energy, India (2 MW 64 phased array), RFMD and Filtronics Compound Semiconductor, U.K. (MMIC radios, PAs), and Milmega UK (GaN PA MMICs, systems). He is currently with Sony Europe B.V. U.K., as the Chief Technologist- microwave and mmW and Tech. Lead nextgeneration/5G front-end modules. He is highly motivated to innovative multidisciplinary industrial R&D, and in the field of advanced multilayer/3D mmW integration and packaging, and very high-power amplifier, recently, he has delivered more than 50 invited keynote/special talks in IEEE conferences.

Dr. Samanta was the recipient of the Commonwealth Fellowship in 2003, Best International Researcher Award in 2005, and Engineering Excellence Award from the IET (IEE) in London, in 2005. He is a Fellow of IET and a Life Fellow of IETE, Chair/Member of IEEE MTT-S Tech Committees - TC-16 (packaging and interconnects), TC-12 (high power/PA), TC-14 (MMIC/MCM), TC-5 (filters/passives), and HIR 5G-AMS Working Group. He sits on the TPC of the main IEEE MTTS conferences. He was an Associate Editor (AE) for IEEE MWCL during 2013–2018. He is also an AE for *IEEE Microwave Magazine*, IET MAP, and IEEE TRANSACTIONS ON MICROWAVE THEORY AND TECHNIQUES, and the Topic Editor of IEEE JOURNAL MICROWAVES.